

石墨烯导热材料研究进展

Research progress in graphene based thermal conductivity materials

李 岳^{1,2}, 李炯利^{1,2,3}, 朱巧思^{1,2}, 梁佳丰^{1,2}, 郭建强^{1,2,3}, 王旭东^{1,2,3},

(1 中国航发北京航空材料研究院, 北京 100095;

2 北京石墨烯技术研究院有限公司, 北京 100094;

3 北京市石墨烯及应用工程技术研究中心, 北京 100095)

LI Yue^{1,2}, LI Jiong-li^{1,2,3}, ZHU Qiao-si^{1,2}, LIANG Jia-feng^{1,2},

GUO Jian-qiang^{1,2,3}, WANG Xu-dong^{1,2,3}

(1 AECC Beijing Institute of Aeronautical Materials, Beijing 100095,
China; 2 Beijing Institute of Graphene Technology, Beijing

100094, China; 3 Beijing Engineering Research Centre
of Graphene Application, Beijing 100095, China)

摘要: 石墨烯作为一种具有超高热导率的二维纳米材料, 在导热领域有着广阔的应用前景。本文综述了石墨烯导热材料的研究进展, 介绍了石墨烯本征热导率及其层数、缺陷、边缘情况等对热导率的影响, 分析了石墨烯纤维的研究现状及存在的问题, 讨论了各类石墨烯导热薄膜(纯石墨烯薄膜/石墨烯杂化薄膜/石墨烯聚合物复合薄膜)热导率的影响因素, 归纳总结了各类三维石墨烯导热材料(无规分散石墨烯三维复合材料和特定结构石墨烯三维复合材料)的结构、性能与研究现状, 最后指出了目前几种导热材料研究存在的问题并展望了石墨烯未来导热领域的发展方向, 尤其是在 LED 照明、智能手机等高功率、高度集成系统中, 石墨烯导热材料有着良好的发展前景。

关键词: 石墨烯; 热导率; 石墨烯纤维; 石墨烯薄膜; 三维石墨烯; 石墨烯基复合材料

doi: 10.11868/j.issn.1001-4381.2020.000935

中图分类号: TB34 **文献标识码:** A **文章编号:** 1001-4381(2021)11-0001-13

Abstract: As a two-dimensional (2D) building block of new materials, graphene has received widespread attention due to its exceptional thermal properties. The thermal properties and recent advances on graphene-based material were reviewed. The intrinsic thermal conductivity of graphene and the effect of layers, defects and edge were briefly introduced. The resent research progress in graphene fiber as thermal conductivity material was analyzed and discussed. A variety of graphene films (graphene film, graphene hybrid film, graphene/polymer composite film) were grouped by category and the influencing factors of the thermal conductivity were reviewed. The structure, thermal conductivity property and current researches of 3D graphene (graphene with random orientation in the polymer matrix, graphene with specific orientation in the polymer matrix) were summarized. Finally, the challenges and prospects of graphene-based materials were also pointed out, especially inhigh power, highly integrated systems such as LED lighting and smart phones, graphene based thermal conductivity materials have a good development prospect.

Key words: graphene; thermalconductivity; graphene fiber; graphene film; 3D graphene; graphene based composite

随着电子电器设备向大容量、高功率密度和小型

轻量化发展, 小空间和大功率会不可避免地产生大量热量聚集, 温度升高会降低电子电器设备性能及减少使用寿命, 并带来安全隐患。为满足目前的市场需求, 人们致力于寻求新型的高效导热材料来改善散热问

题^[1-2]。

石墨烯是碳原子以 sp^2 杂化组成的二维纳米材料, 具有超高的电导率($2000 \text{ S} \cdot \text{m}^{-1}$)、杨氏模量(1 TPa)、断裂强度(130 GPa)^[3-4], 热导率高达 $5300 \text{ W} \cdot \text{m}^{-1} \cdot \text{K}^{-1}$, 远高于同属碳材料的金刚石($2000 \text{ W} \cdot \text{m}^{-1} \cdot \text{K}^{-1}$)与

碳纳米管(单壁 $3500 \text{ W} \cdot \text{m}^{-1} \cdot \text{K}^{-1}$)^[5], 基于石墨烯的高导热材料引起了国内外广泛关注^[6-8]。本文对石墨烯的本征热导率及其影响因素进行了讨论,介绍了目前以石墨烯作为主体材料的导热材料,包括石墨烯纤维、石墨烯薄膜和三维石墨烯,分析了它们的热导率及各类影响因素,探讨现有研究中存在的问题,并展望了其未来的发展前景。

1 石墨烯本征热导率及其影响因素

1.1 石墨烯本征热导率

2008年,为了精准测量石墨烯的本征热导率,Balandin等^[9]将石墨进行机械剥离,制备出单层石墨烯,将其悬浮于Si/SiO₂基底凹槽上,采用非接触式光热拉曼的方法测量了单层石墨烯的热导率,如图1所示,悬浮于沟槽上的单层石墨烯中央部分被激光加热,产生局部热点并在单层石墨烯片层内部传播,通过拉曼G峰值对应的频率对激发激光功率的依赖性得出,单层石墨烯在室温下的热导率为4840~5300 $\text{W} \cdot \text{m}^{-1} \cdot \text{K}^{-1}$ 。2010年,Cai等^[10]也采用光热拉曼法,对沉积在Cu箔上的单层石墨烯行了测试,在350 K的条件下,热导率为2500 $\text{W} \cdot \text{m}^{-1} \cdot \text{K}^{-1}$ 左右,Xu等^[11]同样对沉积在Cu箔上的单层石墨烯进行了测试,在300 K下,热导率为1689~1813 $\text{W} \cdot \text{m}^{-1} \cdot \text{K}^{-1}$,这种非接触式显微拉曼光谱模型也是测试单层石墨烯热导率最常用的方法。

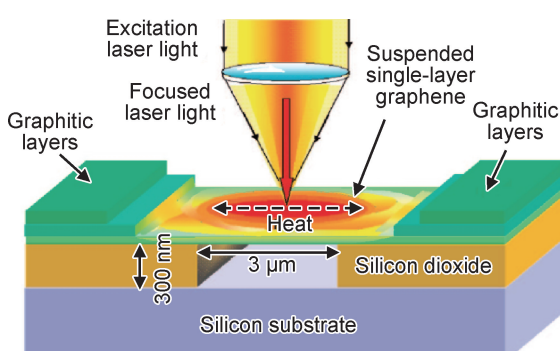


图1 激发激光聚焦在悬浮于沟槽的石墨烯片上的实验示意图^[9]

Fig. 1 Schematic of the experiment showing the excitation laser light focused on a graphene layer suspended across a trench^[9]

1.2 石墨烯本征热导率影响因素

1.2.1 层数

石墨烯的层数对其热导率有很大影响,单层石墨烯在发生热传导时,声子的传播没有横向分量,随着石墨烯层数增加,声子散射产生横向分量,从片层顶部到底部存在边界散射,热导率降低,渐渐接近石墨^[12]。

Ghosh等^[13]研究了石墨烯层数对本征热导率的影响,他们采用机械剥离高取向热解石墨,发现当石墨烯的原子层数从2增加到4时,热导率由2800 $\text{W} \cdot \text{m}^{-1} \cdot \text{K}^{-1}$ 减少到1300 $\text{W} \cdot \text{m}^{-1} \cdot \text{K}^{-1}$,这是由于随着石墨烯片层的增加,片层之间会存在空隙造成声子散射,导致热导率降低。Fugallo等^[14]得出单层石墨烯、双层石墨烯以及天然石墨的热导率分别为3600, 2200, 2000 $\text{W} \cdot \text{m}^{-1} \cdot \text{K}^{-1}$,可以发现,随着石墨烯层数增加,热导率呈下降趋势。Nayandep等^[15]采用闪点法对层数为30~45石墨烯纳米片进行表征,热导率为2180~275 $\text{W} \cdot \text{m}^{-1} \cdot \text{K}^{-1}$,相比于单层石墨烯而言,它的热导率数值更与石墨接近($2000 \text{ W} \cdot \text{m}^{-1} \cdot \text{K}^{-1}$)。

1.2.2 缺陷

石墨烯缺陷可以分为固有缺陷和外部引入缺陷两类,固有缺陷由碳原子非正常排布造成,主要包括点缺陷与空位缺陷,晶界及线缺陷两种形式。

石墨烯中的点缺陷是指由碳-碳单键旋转而产生的相邻的五边形和七边形环对,这种缺陷的生成不涉及碳原子引入或缺失。单空位缺陷是指石墨烯六元碳环中损失一个碳原子,在单空位缺陷的基础上,如果再丢失碳原子,就会产生多空位缺陷,碳原子的缺失会造成区域结构重排,这种结构缺陷会成为热流散射的中心,削弱石墨烯的热耗散能力,导致本征热导率降低。Malekpour等^[16]采用低能电子束辐照石墨烯,在石墨烯片层上制造空穴缺陷,在室温下,随着片层缺陷密度从 $2.0 \times 10^{10} \text{ cm}^{-2}$ 上升到 $1.8 \times 10^{11} \text{ cm}^{-2}$,石墨烯的热导率从 $1800 \text{ W} \cdot \text{m}^{-1} \cdot \text{K}^{-1}$ 下降到 $400 \text{ W} \cdot \text{m}^{-1} \cdot \text{K}^{-1}$ 。Justin等^[17]通过分子动力学计算发现,当石墨烯具有0.1%的点缺陷时,热导率较原来下降69%,而存在0.1%的单空位缺陷和双空位缺陷时,热导率分别降低81%和69%。

通过化学气相沉积方法制备的石墨烯形成空位缺陷的概率较小,但石墨烯在基体的不同位置同时生长时会产生不同二维空间取向,当不同取向片层交叉融合时,会形成由五边形或者八边形组成的线缺陷,也可能在片层锯齿形方向上形成晶界^[18]。Serov等^[19]采用非平衡格林公式计算发现,当采用化学气相沉积制备石墨烯片存在线缺陷时,声子传输能力低,热导率显著下降。Bargi等^[20]通过分子动力学计算发现,之字形无缺陷石墨烯的热导率为 $2650 \text{ W} \cdot \text{m}^{-1} \cdot \text{K}^{-1}$,而当石墨烯存在21.7°倾斜的晶界时,热导率降低至 $2380 \text{ W} \cdot \text{m}^{-1} \cdot \text{K}^{-1}$,同样Cao等^[21]也研究了晶界对石墨烯热导率的影响,他们发现当之字形和扶手椅形边界的石墨烯存在约22°倾斜晶界时,热导率分别降低了26%和32%。

石墨烯外部引入缺陷,一是面内杂原子的掺杂,二是面外杂原子的取代缺陷。

当非碳原子取代石墨烯中碳原子的位置,则形成了杂原子掺杂石墨烯,常见的杂原子掺杂主要为氮、硼^[22]。研究者发现,这种硼掺杂和氮掺杂的石墨烯在导电和催化方面有良好的应用前景,但是在导热方面并没有显示出优异的性能,例如 Senturk 等^[23]采用分子动力学模拟计算得出当石墨烯进行 1% (原子分数) 的氮掺杂时,石墨烯的热导率降低约 50%。

Chien 等^[24]采用分子动力学模拟研究发现,外来的氢原子缺陷会导致热导率降低,当氢原子覆盖率小于 5% 时,导热系数呈线性下降,当氢原子覆盖率达到 10% 时,导热率下降了 70%。他们的团队还采用反向非平衡分子动力学计算,发现石墨烯表面存在随机分散的甲基和苯基时,官能团的覆盖度仅为石墨烯的 1.25%,热导率会降低 50%^[25]。在氧化石墨烯制备过程中,石墨烯表面会引入含氧官能团,这些杂原子会通过共价键或弱范德华力与临近的碳原子结合,给石墨烯带来了高密度缺陷^[26],导致热导率急剧降低。采用热还原或还原剂可以在一定程度上修复石墨烯结构缺陷,但被引入的含氧基团很难被完全脱除,尤其是热还原的方法中,氧原子脱除的同时会脱除碳原子产生空洞(1300 °C 以下),形成石墨烯的固有缺陷,限制了本征热导率。Nayandeep 等^[15]采用闪点法对氧化石墨烯(碳含量 46%)进行了测试,热导率仅为(18±2) W·m⁻¹·K⁻¹。图 2 为石墨烯片层上各类缺陷的示意图^[27]。

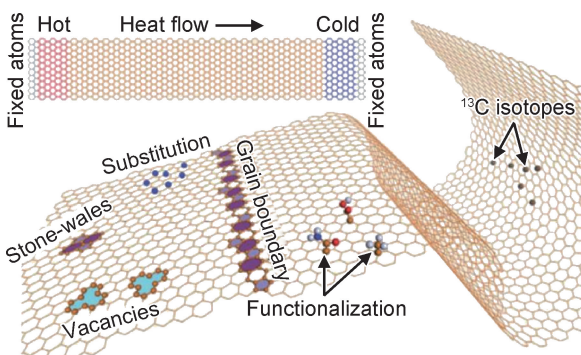


图 2 石墨烯片缺陷示意图^[27]

Fig. 2 Schematic of graphene defects^[27]

1.2.3 粗糙度及边缘形状

粗糙的边缘会导致声子的散射,具有光滑边缘的石墨烯的热导率要高于边缘粗糙的石墨烯,Evans 等^[28]采用分子动力学模拟计算,之字形光滑边缘的石墨烯热导率约为 3000 W·m⁻¹·K⁻¹,而边缘粗糙的石墨烯仅为 800 W·m⁻¹·K⁻¹,同样的,扶手椅边缘的石墨烯也遵循此规律。对于不同边缘形状的石墨烯

而言,之字形边缘的石墨烯比扶手椅状的石墨烯热导率高,这是由于在单位长度下扶手椅式边缘的原子数比之字形边缘原子数量更多,所以声子散射的程度更高。Justin 等^[17]通过分子动力学模拟计算得出具有相同宽度(400 nm)和长度(100 nm)的扶手椅状石墨烯热导率为 680 W·m⁻¹·K⁻¹,而之字形石墨烯为 840 W·m⁻¹·K⁻¹。

1.2.4 基材

Seol 等^[29]采用二氧化硅作为衬底支撑,单层石墨烯的热导率约为 600 W·m⁻¹·K⁻¹,Cai 等^[10]测试得出,采用铜箔作为衬底时,单层石墨烯的热导率降低到 50~1020 W·m⁻¹·K⁻¹。在大多实际应用的电子设备中,石墨烯会被包裹在诸如二氧化硅之类的电介质中,声子在单层石墨烯上进行传输时,由于一个原子层厚度十分小,对表面干扰非常敏感,所以电介质的存在会折损热传输能力。Jang 等^[30]将石墨烯嵌入二氧化硅基体后,热导率为 160 W·m⁻¹·K⁻¹,远远低于其本征热导率。当石墨烯附着在基材上或与聚合物复合后,石墨烯与基材之间存在界面,原本在石墨烯片层上的声子振动传播遇到杂质后会发生散射,使热导率降低。

1.2.5 其他

(1) 聚合物残留

采用化学气相沉积的方法制备石墨烯时,不仅存在多晶界、线缺陷等固有缺陷,石墨烯在转移过程中也会产生聚合物残留,这种杂质的存在会导致热导率降低。例如 Petter 等^[31]采用机械剥离的方法制备了双层石墨烯,使用聚甲基丙烯酸甲酯(PMMA)转移,并用丙酮除去 PMMA 基体,在氢气气氛下高温退火,在透射电镜下发现,丙酮和退火过程并不能完全去除 PMMA,石墨烯片层上含有残留聚合物,热导率仅为 600 W·m⁻¹·K⁻¹。

(2) 同位素取代

当石墨烯表面的¹²C 被同位素¹³C 所取代时,石墨烯的热导率会下降。Chen 团队^[32]通过分子动力学模拟发现,当石墨烯全部由¹²C 组成时,热导率为 2859 W·m⁻¹·K⁻¹,由 99% 的¹²C 和 1% 的¹³C 组成时,热导率为 1855 W·m⁻¹·K⁻¹,而当¹³C 的取代率达到 50% 时,热导率降低到 1151 W·m⁻¹·K⁻¹。

文献中有关石墨烯本征热导率的测试方法及数值具体见表 1^[9-12,14-15]。

2 石墨烯纤维导热材料

石墨烯具有超高的本征热导率,采用石墨烯作为原材料制备连续的高导热宏观结构,如纤维、薄膜是近

表 1 石墨烯的热导率
Table 1 Thermal conductivity of graphene

Sample	Method	Measurement method	Thermal conductivity/ (W · m ⁻¹ · K ⁻¹)	Reference
Suspended single layer graphene	Mechanical cleavage	Confocalmicro-Raman spectroscopy-based measurement	3080-5150	[9]
Suspended graphene on the Au-coated SiN _x porous membrane	Chemical vapor deposition	Confocalmicro-Raman spectroscopy-based measurement	2500	[10]
Suspended single-layer graphene on copper (experimental)	Chemical vapor deposition	Confocalmicro-Raman spectroscopy-based measurement	1800-5300	[11]
Suspended single-layer graphene on copper (theory)	—	Non-equilibrium molecular dynamics simulations	1689-1813	[11]
Suspended high-quality few-layer graphene (the number of atomic planes from 2 to 4)	Mechanical cleavage	Confocalmicro-Raman spectroscopy-based measurement	2800-1300	[12]
Bilayer graphene	—	Model calculation	2200-2500	[14]
Graphene nanoplatelets(interlayer spacing 0.3372 nm)	—	Thermal flash technique	2275±338	[15]
Graphene nanoplatelets(interlayer spacing 0.3376 nm)	—	Thermal flash technique	2180±314	[15]
Graphene oxide	Oxidation	Thermal flash technique	18±2	[15]

年来的热点研究方向。由于没经过表面处理的石墨烯具有很高的化学稳定性,不能够自组装形成宏观结构,而研究发现氧化石墨烯通过还原的方式能够转化为石墨烯,并且在水中具有良好的分散性,能够形成溶质向列液晶,片层预取向,为形成宏观有序的纤维结构奠定了基础。

限制石墨烯纤维的热导率的因素主要集中在以下方面,首先,石墨烯热传导主要来自共价 sp²键合网络,但采用氧化石墨烯作为制备石墨烯纤维的前驱体,片层上的各类晶格缺陷以及残余官能团会导致大量的声子散射。采用大片氧化石墨烯作为原材料更容易获得更大的晶域面积,减少边缘,降低声子散射。高温退火可以去除含氧官能团,修复晶格缺陷,扩大 sp²晶域面积。例如 Xu 等^[33]采用小尺寸的氧化石墨烯且退火温度小于等于 1300 ℃时,纤维中石墨烯的 sp²晶域面积较小,而采用大片氧化石墨烯作为构架纤维的前驱体时,当退火温度从 1300 ℃上升到 3000 ℃,显著提升了石墨烯晶域面积。同时 Xin 团队等^[34]采用大片氧化石墨烯制备纤维,退火温度从 1400 ℃提升到 2850 ℃,轴向和径向的尺寸分别从 40~50 nm 提升到 783 nm 和 423 nm。

其次是取向问题,高度取向可以充分发挥石墨烯片层在轴向方向的导热性能。当二维的石墨烯片层在纺丝管道中流动时,由于管道内的流动剪切应力存在梯度,会产生趋肤效应,靠近管道壁的石墨烯片层的轴向取向度较高,而靠近中心的石墨烯片层排列混乱,形成核壳结构^[35]。Park 等^[36]发现在形成稳定液晶相的

浓度范围内,氧化石墨烯分散液为非牛顿流体,当从狭窄通道流出到扩展区域时,氧化石墨烯片层会发生垂直方向的重新排列,被挤压的片层会向其他方向膨胀。为了抑制片层垂直取向,一般采用两种方法,第一是设计收缩的纺丝通道来控制石墨烯片层在垂直方向上的膨胀现象,其次是对纺好的纤维进行强力拉伸,Xu 等^[33]采用此种方法,使石墨烯在轴向的取向度高达 81%。

其三,石墨烯独特的二维片层结构具有较大的长径比,纤维内部容易发生折叠,形成较大空隙,虽然理想的石墨烯晶体体积密度为 2.2 g · cm⁻³,而从凝固浴中或低温环境中收集的石墨烯纤维内部呈现松散堆积的状态,密度仅为 1 g · cm⁻³,而经过拉伸和高温处理等程序,密度能够提升到大于 1 g · cm⁻³,但仍普遍低于常规碳纤维的密度(1.7~1.9 g · cm⁻³),这是其热导率不理想的重要原因^[35]。

针对以上问题,如图 3 所示,Xin 团队^[34]使用大片氧化石墨烯为原料,采用湿法纺丝制备了石墨烯纤维。针对石墨烯纤维密度问题,Xin 团队加入质量分数为 30% 的小片石墨烯填补内部空隙,使纤维密度上升到 1.8~1.9 g · cm⁻³,接近于碳纤维。而为了修复石墨烯的缺陷,减少声子散射,采用 2850 ℃高温退火,在轴向方向形成了较大的亚微米级晶域,实现了有效的声子传输,热导率高达 1290 W · m⁻¹ · K⁻¹。

采用管状通道纺丝,由于片层和通道的尺寸和几何形状不匹配会导致石墨烯片层褶皱和随机取向,为增强纤维的取向度,Xin 团队^[37]采用扁平且收缩的通

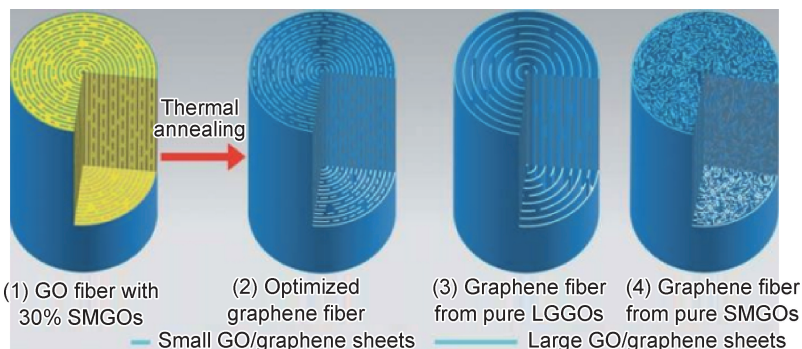
图3 具有大小片层“插入”结构的高导热与高机械强度的石墨烯纤维^[34]

Fig. 3 Highly thermally conductive and mechanically strong graphene fibers with an “intercalated” structure of large and small-sized graphene sheets^[34]

道来制备高取向度石墨烯带状纤维,当氧化石墨烯溶液从宽通道进入窄通道时,随着通道横截面积的减小,流速和剪切应力增加,降低了流体黏度,同时具有高长径比的通道与二维的氧化石墨烯片层具有几何兼容性,优化了片层排列,提高轴向的片层取向度,经过 2500 °C 高温退火,在径向的微晶尺寸能够达到 612 nm,纤维的热导率高达 1575 W · m⁻¹ · K⁻¹。

石墨烯纤维的热导率较单层石墨烯有一定差距,这是由于不连续的片层结构会存在大量的声子散射现象,石墨烯片层在纤维内部褶皱堆叠无法完全伸展并取向,而且制备纤维采用的氧化石墨烯本身具有的各类晶格缺陷难以完全修复,这些是导致石墨烯纤维的热导率低于其本征热导率的根本原因。

3 石墨烯膜导热材料

石墨烯独特的二维片层结构,片层与片层之间存在 π - π 共轭,容易实现紧密有序的层状结构,这种有序的层状结构构建了平面方向的传播路径,有利于声子在平面方向的传播,且石墨烯本征热导率很高,这为薄膜的高面内热导率提供了可能^[33,38-39]。

3.1 石墨烯膜

对于纯石墨烯膜而言,影响热导率的主要因素与

石墨烯纤维基本相同,首先是由于石墨烯表面惰性,不能够自组装成膜,氧化石墨烯存在高密度缺陷,为获得较大的 sp^2 晶域面积,提升薄膜热导率,一般采用大片氧化石墨烯为原料后经高温退火的方法来修复缺陷。其次是不连续的片层结构阻断了声子的传播路径,以及石墨烯片层的褶皱及堆叠现象都会导致片层取向度低,影响薄膜的热导率。在纤维导热的有关文献中,扁平的通道和石墨烯片层具有几何兼容性,纺出的纤维取向度较高,提升了热导率,而对于石墨烯薄膜这种平面材料而言,由于在平面方向没有空间限制,更容易实现石墨烯片层的铺展,促进了平面方向的高取向度,因此可以充分利用面内导热的优势,规避法向导热差的劣势。为了获得高取向度的石墨烯薄膜,一般对薄膜施加机械压力,减少薄膜内部的空穴和褶皱。

Peng 等^[40]指出将退火温度从 1400 °C 上升到 3000 °C 时,薄膜的热导率能够从 720 W · m⁻¹ · K⁻¹ 上升至 1940 W · m⁻¹ · K⁻¹,如图 4 所示,将退火后的石墨烯薄膜采用机械挤压的方式排出含氧官能团还原产生的半富勒烯微气囊,在薄膜内部形成褶皱结构,赋予了薄膜超高的柔韧性,能够承受 100000 次 180° 弯曲循环以及 6000 次的极限折叠。

Wang 等^[41]采用铝基板预还原并结合高温(2850 °C)

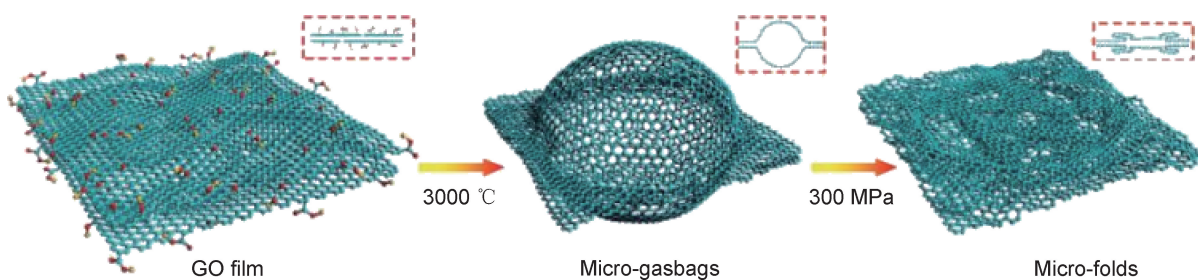
图4 通过微气囊将褶皱引入石墨烯薄膜实验示意图^[40]

Fig. 4 Introducing microfolds to graphene film(GF) via microgasbags^[40]

以及强机械压力制备了高品质石墨烯膜,石墨化后,采用机械压力进一步减少膨胀现象和片层褶皱,增强石墨烯片层沿着面内方向的取向,减少声子散射的问题,最终得到的石墨烯薄膜导热率能够达到 $3200 \text{ W} \cdot \text{m}^{-1} \cdot \text{K}^{-1}$ 。值得一提的是,此时法相热导率仅为 $14.8 \text{ W} \cdot \text{m}^{-1} \cdot \text{K}^{-1}$,表明片层取向对热导率影响很大,同时经过高度还原的氧化石墨烯薄膜在 6000 次 180° 弯曲循环中没有发生破损和断裂,表现出出色的柔韧性。

表 2 为石墨烯和石墨烯相关的薄膜导热率统计^[40-60]。可以看出,经过高温还原后石墨烯膜的热导率目前报道最高能够达到 $3200 \text{ W} \cdot \text{m}^{-1} \cdot \text{K}^{-1}$,与单层石墨烯的热导率相当,甚至高于少层石墨烯纳米片的热导率(可能与测试方法不同有关)。高温处理能够消除相邻石墨烯片层之间的重叠,从最初的无机堆叠的氧化石墨烯片转变为平坦连续的石墨烯层,为声子传输提供有效路径^[61]。

3.2 石墨烯复合/杂化薄膜

Zou 等^[42]将氧化石墨烯溶液与聚多巴胺溶液混

合进行抽滤,多巴胺表面氨基与氧化石墨烯片层上的含氧基团具有氢键作用,同时石墨烯片层与多巴胺也存在 $\pi-\pi$ 共轭,经过 3000°C 高温退火,制备得到热导率高达 $1584 \text{ W} \cdot \text{m}^{-1} \cdot \text{K}^{-1}$ 的无定形碳石墨烯导热薄膜。类似的,将聚酰胺酸接枝到石墨烯表面,经过低温聚合,制备得到石墨烯聚酰亚胺复合薄膜, 2800°C 高温炭化后,得到薄膜热导率高达 $1352 \text{ W} \cdot \text{m}^{-1} \cdot \text{K}^{-1}$ ^[43]。

对于石墨烯复合薄膜,Wang 等^[44]采用溶胶-凝胶的方法将聚苯撑苯并二恶唑纳米纤维与石墨烯纳米片组装成类珍珠层状结构,这种导热薄膜具有 $45.5 \text{ MJ} \cdot \text{m}^{-3}$ 的良好韧性和 33.6% 的应变失效,同时具有 $130 \text{ W} \cdot \text{m}^{-1} \cdot \text{K}^{-1}$ 的热导率。Feng 等^[45]将氧化石墨烯与天然橡胶复合,这种复合导热薄膜的水平热导率能够达到 $20.84 \text{ W} \cdot \text{m}^{-1} \cdot \text{K}^{-1}$,并且能够承受 10000 次拉伸循环,具有较好的柔韧性。

如表 2 所示,石墨烯复合/杂化导热膜较高温还原的纯石墨烯膜还存在一定差距,其他物质的本征热导率低于石墨烯,他们的加入会降低薄膜的热导率。

表 2 石墨烯和石墨烯相关的薄膜导热率统计

Table 2 Statistics of thermal conductivity of graphene and graphene-based film

Sample	In-plane thermal conductivity/ ($\text{W} \cdot \text{m}^{-1} \cdot \text{K}^{-1}$)	Preparation method	Filler	Reference
GFs-1	1940 ± 113	Blade coating	Reduced graphene oxide	[40]
GFs-2	3200	Dry-bubbling	Reduced graphene oxide	[41]
RGO-PDA	1584	Vacuum filtration	Reduced graphene oxide+amorphous carbon	[42]
g-MGO/PI	1352 ± 5	Evaporation induced self-assembly method	Reduced graphene oxide+amorphous carbon	[43]
GNS/PBONF	≈ 130	Sol-gel	Graphene+poly(p-phenylene benzobisoxazole)	[44]
RGO/NR	20.84	Casting and drying	Reduced graphene oxide+nature rubber	[45]
RGO film-1	61.8	Casting and drying	Reduced graphene oxide	[46]
PGF	1204 ± 35	Blade coating	Reduced graphene oxide	[47]
PG film	803.1	Casting and drying	Reduced graphene oxide	[48]
GO film	≈ 1100	Evaporation of GO suspension	Reduced graphene oxide	[49]
SG2800	2292 ± 159	Chemical vapor deposition	Reduced graphene oxide	[50]
RGO film-2	118.7	3D printing	Reduced graphene oxide	[51]
GP	2600 ± 300	Blade coating	Reduced graphene oxide	[52]
EGF	242	Ball milling+Vacuum filtration	Reduced graphene oxide	[53]
GPF	13.42	Solution based approaches	Reduced graphene oxide+amorphous carbon	[54]
F-graphene/PVA	61.3	Vacuum filtration	Fluorinated graphene+poly(vinylalcohol)	[55]
HAD-g-GN	3.957	Vacuum filtration	Hexadecyl lacrylate-grafted graphene	[56]
RGO/CNR	1820.4	Evaporation-induced self-assembly	Reduced graphene oxide+carbonized into nanorod	[57]
RGO-1/NFC	6.168	Vacuum filtration	Reduced graphene oxide+nanofibrillated cellulose	[58]
RGO-2/NFC	12.6	Layer-by-layer assembly	Reduced graphene oxide+nanofibrillated cellulose	[59]
RGO-3/NFC	9.0	Vacuum filtration	Reduced graphene oxide+nanofibrillated cellulose	[60]

4 石墨烯导热复合材料

聚合物具有轻质、良好的耐腐蚀性及韧性、优异的加工性能和低成本等优势,适应不同形状的界面导热

要求,具备目前所需的导热材料基体的大部分特性,但由于聚合物本身热导率很低,基本在 $0.2 \text{ W} \cdot \text{m}^{-1} \cdot \text{K}^{-1}$ 左右,通常将其与高导热填料进行复合以改善导热率^[62]。石墨烯是热导率最高的纳米材料之一,其独特

的二维片层结构能够提供多渠道声子传输,远超过常规的导热填料如氧化铝($30 \text{ W} \cdot \text{m}^{-1} \cdot \text{K}^{-1}$)、氮化铝($320 \text{ W} \cdot \text{m}^{-1} \cdot \text{K}^{-1}$)、氮化硼($180 \text{ W} \cdot \text{m}^{-1} \cdot \text{K}^{-1}$)等,被广泛用于制备导热复合材料。

4.1 石墨烯在树脂基体中无规分散

目前关于石墨烯在树脂基体中无规分散主要集中在导热填料的研究,通过选择不同的导热填料来改善复合材料的热导率。

4.1.1 氧化石墨烯

石墨烯本身具有轻质、低密度的特性,在较低的填料含量下就会导致树脂的黏度上升,所以在聚合物中填充量并不大。将氧化石墨烯直接与环氧树脂基体复合,填料质量分数为 10% 时,Song 等^[63]得出复合材料的热导率约为 $0.75 \text{ W} \cdot \text{m}^{-1} \cdot \text{K}^{-1}$ 。Zong 等^[64]将质量分数 0.5% 的氧化石墨烯填入环氧树脂,得到约 $0.26 \text{ W} \cdot \text{m}^{-1} \cdot \text{K}^{-1}$ 的热导率。

由于氧化石墨烯本征热导率较低,仅为 $2 \sim 18 \text{ W} \cdot \text{m}^{-1} \cdot \text{K}^{-1}$,以其作为导热填料制备的复合材料热导率没有明显改善。

4.1.2 还原氧化石墨烯

Ding 等^[65]采用聚合物接枝的方法,使用链端带有活性氨基的聚酰胺-6 与 GO 片发生缩合反应,同时氧化石墨烯发生热还原,填料质量分数为 10% 时,热导率为 $0.42 \text{ W} \cdot \text{m}^{-1} \cdot \text{K}^{-1}$ 。Tang 等^[66]采用生物基聚酯与氧化石墨烯接枝,再使用维生素 C 还原氧化石墨烯,在体积分数为 1.45% 的填料含量下,复合材料的热导率为 $0.54 \text{ W} \cdot \text{m}^{-1} \cdot \text{K}^{-1}$ 。Oh 等^[67]采用硅烷偶联剂对还原氧化石墨烯改性后,与环氧树脂复合,在填料含量为 7% 时,热导率为 $0.75 \text{ W} \cdot \text{m}^{-1} \cdot \text{K}^{-1}$ 。Teng 等^[68]将氧化石墨烯在 1000°C 下还原,得到的还原氧化石墨烯与环氧树脂复合,填料质量分数为 4% 时,热导率约为 $1.55 \text{ W} \cdot \text{m}^{-1} \cdot \text{K}^{-1}$ 。由此可见,采用还原氧化石墨烯作为导热填料时,热导率仍然维持在较低的水平,对比氧化石墨烯复合材料,热导率没有明显提升,相比于目前的传统热填料不具备优势。

4.1.3 高质量石墨烯

由于氧化石墨烯与还原氧化石墨烯的本征热导率的限制,直接采用高品质石墨烯(石墨烯纳米片,热导率在 $2000 \text{ W} \cdot \text{m}^{-1} \cdot \text{K}^{-1}$ 以上,远高于氧化石墨烯及其他常规填料)与树脂基体复合是重要的研究方向。Wang 等^[69]将石墨烯纳米片与环氧树脂复合,当填料质量分数为 5% 时,复合材料的热导率约为 $0.45 \text{ W} \cdot \text{m}^{-1} \cdot \text{K}^{-1}$ 。Zhu 等^[70]采用超声和铸造成型法制备出的石墨烯纳米片环氧树脂复合材料,在填料质量

分数为 4.3% 的情况下,热导率能够达到 $1.06 \text{ W} \cdot \text{m}^{-1} \cdot \text{K}^{-1}$ 。Kim 团队^[71]采用熔融混合工艺将石墨烯纳米片与环氧树脂复合,在填料质量分数为 20% 时,复合材料的热导率约为 $1.5 \text{ W} \cdot \text{m}^{-1} \cdot \text{K}^{-1}$ 。可以看出,在无规分散体系中,采用高品质石墨烯作为导热填料仍不能达到理想的热导率。除了石墨烯本征热导率的因素以外,很多学者认为,复合材料的热导率与石墨烯在树脂基体中的取向、分散能力和界面结合力息息相关。

石墨烯片层容易在聚合物中团聚,与树脂结合能力差^[72-74]。通过表面改性可以解决石墨烯在聚合物中的分散和界面问题^[75-76]。氧化石墨烯的本征热导率太低,为了保证石墨烯的品质、减少缺陷,Song 等^[63]将液相剥离的石墨烯进行非共价改性,与环氧树脂复合,在填料质量分数为 10% 的情况下,热导率为 $1.53 \text{ W} \cdot \text{m}^{-1} \cdot \text{K}^{-1}$ 。非共价改性采用了较高品质石墨烯作为导热填料的同时也改善了石墨烯与树脂基体间的界面结合力,但热导率仍不理想。在规分散体系中,石墨烯片层在基体内部没有形成连通的导热网络,覆盖在石墨烯片层周围的聚合物链阻碍了声子震动传播,热导率处于较低数值^[77-83]。

4.2 特定结构石墨烯分散

由以上无规分散体系的导热结果可以看出,不连续的导热通路会导致复合材料热导率低下。由典型的导热通路理论模型可知,聚合物复合材料的导热机理是在机体内形成导热路径,当填料含量达到逾渗阈值(形成连续导热链的临界值)时,导热粒子形成贯穿整个聚合物基体的局部导热链或导热网,使声子在聚合物体系中更多地沿着连续的石墨烯网络振动传播,材料才会显示出良好的导热率^[84]。

石墨烯在基体中的特定取向主要包括隔离结构与三维结构。隔离结构的制备方法主要是将树脂基体直接与石墨烯粉体混合,之后进行热压成型^[85-86]。制备三维结构的石墨烯主要包括自组装技术,例如水热法或溶胶-凝胶法^[87-88],之后进行冷冻干燥来获得三维石墨,另外还有采用模板法,在三维结构表面负载石墨烯,之后进行模板刻蚀,比如在镍泡沫表面通过化学气相沉积生长石墨烯,之后对镍泡沫进行刻蚀,即制备得到完整的三维结构^[89]。迄今为止,已经将多种三维石墨烯,比如海绵、泡沫和气凝胶掺入树脂基体中,来获得高导热复合材料。

4.2.1 隔离结构

隔离结构是采用石墨烯纳米片与树脂基体直接混合来制备具有三维连通网络的复合材料。

Alam 等^[85]将石墨烯纳米片与聚丙烯(PP)在乙

醇中混合,石墨烯纳米片物理吸附于聚合物微粒的表面,进行干燥后,热压即得到具有隔离结构的 GNP/PP 复合材料,在相同的石墨烯填料含量下,具有这种隔离结构的石墨烯骨架与 PP 的复合材料比采用熔融共混的无机分散的石墨烯/PP 复合材料热导率高出两倍。Wu 等^[86]将多壁碳纳米管(MWCNT)与聚苯乙烯(PS)熔融混合,将复合材料粉碎成微米大小的颗粒,由于存在 π - π 共轭的作用,石墨烯纳米片直接将微米级粉料包裹起来,在高温下热压成型,即制备得到 GNP/MWCNT/PS 三维隔离双网络复合材料,由于 MWCNT 的存在有效增加了导热网络密度,与石墨烯纳米片起到协同作用,复合材料的热导率约为 $1 \text{ W} \cdot \text{m}^{-1} \cdot \text{K}^{-1}$ 。

在以上研究中,虽然采用了本征热导率较高的石墨烯纳米片作为导热填料,但是热导率仍在 $2 \text{ W} \cdot \text{m}^{-1} \cdot \text{K}^{-1}$ 以下。在隔离结构中,石墨烯只是实现了片层的简单搭

接,片层相互之间连接不够紧密,造成声子散射,热导率并不理想。

4.2.2 三维结构

石墨烯预先形成三维结构,有效保证了复合材料中导热网络的完整,相比于石墨烯片层无规分散的复合材料,热导率提升显著。

(1) 无取向(各向同性)

无取向排列指的是在树脂机体内,石墨烯呈现各向同性排布,具有三维连通的导热网络。

如图 5 所示,Liu 等^[90]采用聚酰亚胺大分子连接还原氧化石墨烯片,经过 2800°C 高温石墨化后制备了三维石墨烯气凝胶,聚酰亚胺炭化后形成乱层碳,起到连接石墨烯片层的作用,完善了三维石墨烯气凝胶的内部导热通路。与环氧树脂复合后,填料质量分数为 2.20% 时,其热导率能够达到 $4.56 \text{ W} \cdot \text{m}^{-1} \cdot \text{K}^{-1}$ 。

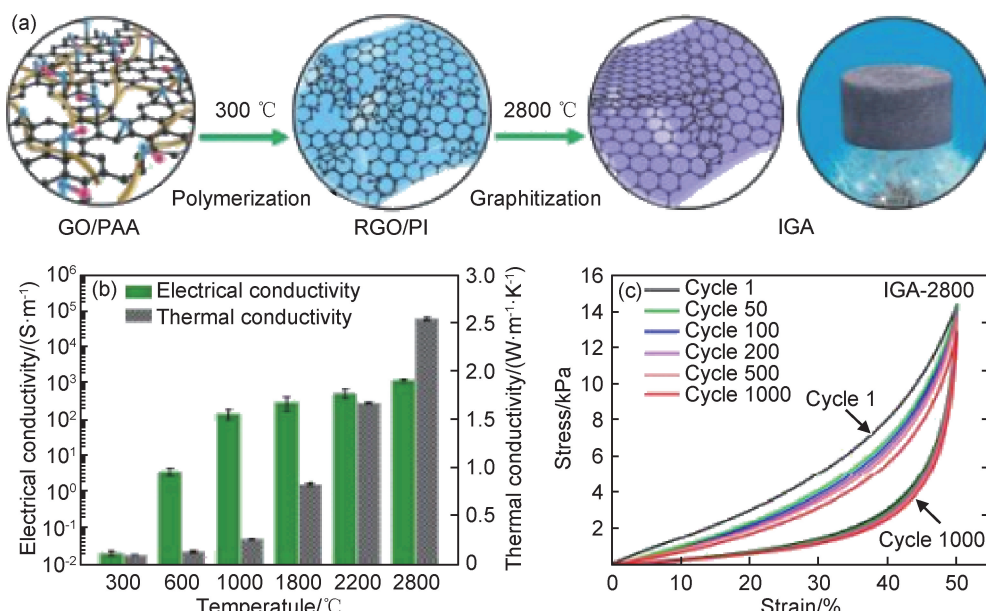


图 5 IGA 的制备及其热导率与力学性能^[90]

(a)GO/PAA 和 RGO/PI 气凝胶制备过程示意图;(b)IGA0.22(氧化石墨与聚酰胺酸初始投料比为 0.22)导电率和石蜡/IGA 复合材料热导率与退火温度的关系图;(c)IGA0.22-2800(氧化石墨与聚酰胺酸初始投料比为 2.2,煅烧温度为 2800°C)在不同应变下的应力-应变曲线

Fig. 5 Fabrication of IGA and their thermal conductivity and mechanical performance^[90]

(a)schematic illustration for fabricating IGA from GO/PAA and RGO/PI aerogels;(b)plots of electrical conductivity of IGA0.22 (initial GO/PAA ratio is 0.22) and thermal conductivity of paraffin/IGA composites versus annealing temperature;(c)stress-strain curves of IGA0.22-2800 (initial GO/PAA ratio is 0.22, thermally treating temperature is 2800°C) with different set strains

除自组装的方法外,高品质石墨烯来构建三维连通网络也可以采用模板法,如 Zhang 等^[91]采用碳纳米管海绵作为模板,在其表面包覆聚酰亚胺,经过高温炭化后,石墨烯能够桥连不连续的碳纳米管海绵,形成完善的三维结构,再通过逐步涂覆聚酰亚胺,制备出的三

维导热复合材料具有高导电、高回弹的特性,同时热导率能够达到 $3.24 \text{ W} \cdot \text{m}^{-1} \cdot \text{K}^{-1}$ 。

(2) 有取向(各向异性)

当片层在三维网络中呈取向排布时,热导率呈现显著的各向异性特征,当沿着片层取向方向进行

热导率表征,由于导热网络在测试方向上是连续通路,热导率较高,而当测试方向为垂直于片层取向方向时,由于片层间存在间隙,导热网络并不完善,热导率较低。

An 等^[88]将高品质石墨烯片和氧化石墨烯共同进行水热反应,得到具有取向结构的高密度三维石墨烯,经过退火处理后与环氧树脂进行复合,沿着片层取向进行测试,热导率能够达到 $35.5 \text{ W} \cdot \text{m}^{-1} \cdot \text{K}^{-1}$,而垂直于片层取向的热导率较低,为 $17 \text{ W} \cdot \text{m}^{-1} \cdot \text{K}^{-1}$ 左右。Min 等^[92]将氧化石墨烯溶液与聚酰胺酸混合,经过双向冷冻制备了具有取向结构的三维石墨烯气凝胶,经过 2800°C 的高温煅烧后,将其与石蜡复合,纵向热导率为 $8.87 \text{ W} \cdot \text{m}^{-1} \cdot \text{K}^{-1}$,横向热导率仅为 $2.68 \text{ W} \cdot \text{m}^{-1} \cdot \text{K}^{-1}$ 。

$\text{W} \cdot \text{m}^{-1} \cdot \text{K}^{-1}$ 。Wu 等^[93]采用插层剥离的石墨烯片与天然橡胶混合,浇注到化学气相沉积制备的石墨烯泡沫中,硫化压力为 10 MPa 时,插层石墨烯在聚合物基体中取向排列,在体积分数为 10% 的填料含量下,复合材料的热导率在沿片层方向能够达到 $11.16 \text{ W} \cdot \text{m}^{-1} \cdot \text{K}^{-1}$,而垂直于片层方向的热导率约为 $4 \text{ W} \cdot \text{m}^{-1} \cdot \text{K}^{-1}$ 。

从以上实例以及图 6 的热导率增强率对比中可以发现,较粉体填料而言,具有特定结构石墨烯的热导率增强率普遍较高^[94-97],这是由于连通的三维结构可以减少界面声子散射,同时采用高质量的石墨烯来构建三维网络,能够进一步提升热导率^[98-100],并且当片层在聚合物基体中取向排布,在沿着片层方向上的热导率较高^[101-105]。

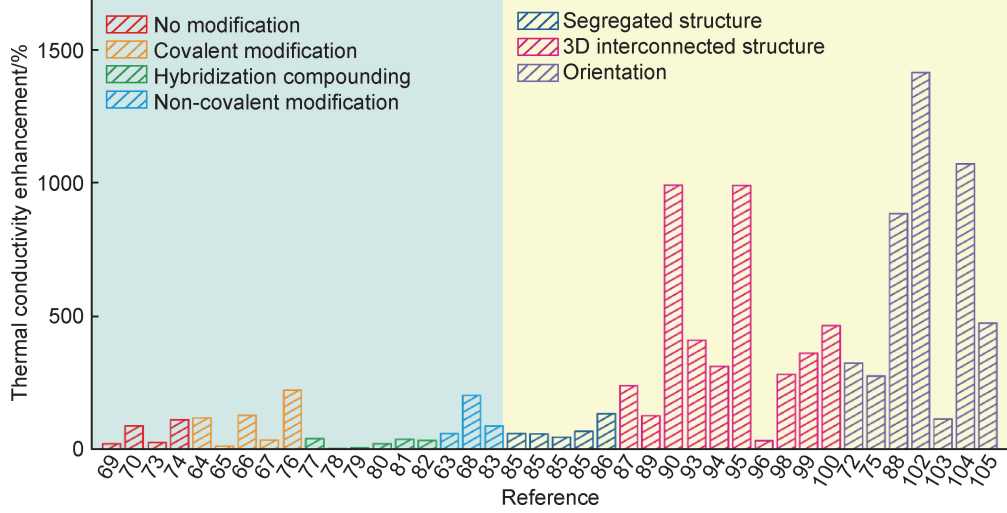


图 6 无规分散和特殊结构石墨烯聚合物复合材料的热导率增强率柱状对比图
Fig. 6 Comparison of thermal performance of polymer composites with dispersed and 3D interconnected fillers in terms of thermal conductivity enhancement

5 结束语

本文总结了石墨烯在导热领域的研究现状,介绍了石墨烯本征热导率,总结了各类宏观石墨烯材料如石墨烯纤维、石墨烯薄膜及三维石墨烯在导热领域的研究进展。

对于石墨烯的本征热导率而言,影响因素包括层数、缺陷、边缘形状及粗糙度及测试手段等,单层悬浮石墨烯的热导率很高,但针对实际应用,将石墨烯制备成宏观的导热材料是目前的热点研究方向。

在石墨烯纤维与薄膜导热材料方面,影响热导率的因素比较一致,主要为缺陷、取向以及片层不连续的问题。由于两种导热材料一般采用氧化石墨烯作为前驱体,本身具有高密度缺陷,采用高温还原能够很大程度上还原氧化石墨烯,但其缺陷并不能完全修复,同时

片层具有较大的径厚比,在制备纤维及薄膜的过程中容易形成褶皱,影响取向度,造成声子散射,导致热导率降低。在纤维方面,片层褶皱不仅影响轴向取向,也会产生空隙降低纤维密度,通过设计纺丝通道的形状及对纤维施加拉伸力或通过叠加大小片石墨烯的方式可以改善上述问题,但石墨烯的二维片层和纤维结构具有几何不兼容性,采用石墨烯制备纤维必然会折损其本征热导率。在石墨烯膜方面,采用对薄膜施加机械压力的方法,能够提高平面取向度,得到的膜材料热导率接近于石墨烯纳米片的本征热导率。

在三维石墨烯导热复合材料方面,热导率同样也取决于石墨烯片的缺陷程度及片层取向。当石墨烯片层在树脂基体中无规分散时,即使使用高质量石墨烯改善分散与界面问题,复合材料的热导率也提升有限。当采用氧化石墨烯进行自组装或者采用模板法制备三

维石墨烯导热网络,再浸润树脂制备导热复合材料时,热导率显著高于无规分散的石墨烯聚合物复合材料,并呈现各向异性特征,沿着石墨烯片取向方向上具有更高的热导率。

综上所述,虽然石墨烯在导热领域研究取得了很大的进展,但是在实际应用方面仍处于初期阶段,尽管如此,石墨烯导热薄膜及取向型三维石墨烯导热复合材料仍具有良好的应用前景。目前市面上不乏石墨烯导热相关产品,例如应用于华为手机上的石墨烯散热膜以及应用于照明领域的 LED 石墨烯散热涂层等,随着不断探索,石墨烯会为导热事业带来巨大助力。

参考文献

- [1] YU A P, RAMESH P, SUN X B, et al. Enhanced thermal conductivity in a hybrid graphite nanoplatelet-carbon nanotube filler for epoxy composites[J]. Advanced Materials, 2008, 20(24): 4740-4744.
- [2] KIM H S, JANG J U, LEE H, et al. Thermal management in polymer composites: a review of physical and structural parameters[J]. Advanced Engineering Materials, 2018, 20(10): 1800204.
- [3] ZHANG Y, TAN Y W, STORMER H L, et al. Experimental observation of the quantum Hall effect and Berry's phase in graphene[J]. Nature, 2005, 438(7065):201-204.
- [4] NAIR R P, BLAKE P, GRIGORENKO A N, et al. Fine structure constant defines visual transparency of graphene[J]. Science, 2008, 320(5881):1308.
- [5] HUANG X Y, IIZUKA T, JIANG P K, et al. Role of interface on the thermal conductivity of highly filled dielectric epoxy/AlN composites[J]. The Journal of Physical Chemistry C, 2012, 116(25):13629-13639.
- [6] 段森,李四中,陈国华. 机械法制备石墨烯的研究进展[J]. 材料工程, 2013(12):85-91.
- DUAN M, LI S Z, CHEN G H. Research progress in preparation of graphene by mechanical exfoliation[J]. Journal of Materials Engineering, 2013(12), 85-91.
- [7] 钱伟,何大平,李宝文. 石墨烯基电磁屏蔽材料的研究进展[J]. 材料工程, 2020, 48(7):14-23.
- QIAN W, HE D P, LI B W. Recent progress on graphene-based materials for electromagnetic interference shielding applications [J]. Journal of Materials Engineering, 2020, 48(7):14-23.
- [8] 白明洁,刘金龙,齐志娜,等. 石墨烯纳米流体研究进展[J]. 材料工程, 2020, 48(4):46-59.
- BAI M J, LIU J L, QI Z N, et al. Research progress in nanofluids with graphene addition [J]. Journal of Materials Engineering, 2020, 48(4):46-49.
- [9] BALANDIN A A, GHOSH S, BAO W Z, et al. Superior thermal conductivity of single-layer graphene [J]. Nano Letters, 2008, 8(3):902-907.
- [10] CAI W, MOORE A L, ZHU Y, et al. Thermal transport in suspended and supported monolayer graphene grown by chemical vapor deposition[J]. Nano Letters, 2010, 10(5):1645-1651.
- [11] XU X, PEREIRA L F, WANG Y, et al. Length-dependent thermal conductivity in suspended single-layer graphene[J]. Nature Communications, 2014, 5:3689.
- [12] GHOSH S, BAO W, NIKA D L, et al. Dimensional crossover of thermal transport in few-layer graphene[J]. Nature Materials, 2010, 9(7):555-558.
- [13] GHOSH S, CALIZO I, TEWELDEBRHAN D, et al. Extremely high thermal conductivity of graphene: prospects for thermal management applications in nanoelectronic circuits[J]. Applied Physics Letters, 2008, 92(15):151911.
- [14] FUGALLO G, CEPELLOTTI A, PAULATTO L, et al. Thermal conductivity of graphene and graphite: collective excitations and mean free paths[J]. Nano Letters, 2014, 14(11): 6109-6114.
- [15] NAYANDEEP K M, ALEXIS R A. Thermal conductivity of graphene and graphene oxide nanoplatelets[J]. IEEE, 2012.
- [16] MALEKPOUR H, RAMNANI P, SRINIVASAN S, et al. Thermal conductivity of graphene with defects induced by electron beam irradiation [J]. Nanoscale, 2016, 8 (30): 14608-14616.
- [17] JUSTIN H, ALPER K, CEM S, et al. Control of thermal and electronic transport in defect-engineered graphene nanoribbons [J]. ACS Nano, 2011, 5(5):3779-3787.
- [18] FLORIAN B, JANIK K, ARKADY V K. Structural defects in graphene[J]. ACS Nano, 2011, 5(1):26-41.
- [19] SEROV A Y, ONG Z Y, POP E. Effect of grain boundaries on thermal transport in graphene[J]. Applied Physics Letters, 2013, 102(3):033104.
- [20] BARGI A, KIM S P, RUOFF R S, et al. Thermal transport across twin grain boundaries in polycrystalline graphene from nonequilibrium molecular dynamics simulations[J]. Nano Letters, 2011, 11(9):3917-3921.
- [21] CAO A J, QU J M. Kapitza conductance of symmetric tilt grain boundaries in graphene[J]. Journal of Applied Physics, 2012, 111(5):053529.
- [22] WEI D C, LIU Y Q, WANG Y. Synthesis of N-doped graphene by chemical vapor deposition and its electrical properties[J]. Nano Letters, 2009, 9:1752-1758.
- [23] SENTURK A E, OKTEM A S, KONUKMAN A E S. Effects of the nitrogen doping configuration and site on the thermal conductivity of defective armchair graphene nanoribbons[J]. J Mol Model, 2017, 23(8):247.
- [24] CHIEN S K, YANG Y T, CHEN C K. Influence of hydrogen functionalization on thermal conductivity of graphene: nonequilibrium molecular dynamics simulations [J]. Applied Physics Letters, 2011, 98(3):033107.
- [25] CHIEN S K, YANG Y T, CHEN C K. Influence of chemisorption on the thermal conductivity of graphene nanoribbons[J]. Carbon, 2012, 50(2):421-428.
- [26] 郭建强,李炯利,梁佳丰,等. 氧化石墨烯的化学还原方法与机理研究进展[J]. 材料工程, 2020, 48(7):24-35.

- GUO J Q, LI J L, LIANG J F, et al. Research progress in methods and mechanisms of chemical reduction graphene oxide[J]. *Journal of Materials Engineering*, 2020, 48(7):24-35.
- [27] POP E, VARSHNEY V, ROY A K. Thermal properties of graphene: fundamentals and applications[J]. *MRS Bulletin*, 2012, 37(12):1273-1281.
- [28] EVANS W J, HU L, KEBLINSKI P. Thermal conductivity of graphene ribbons from equilibrium molecular dynamics: effect of ribbon width, edge roughness, and hydrogen termination[J]. *Applied Physics Letters*, 2010, 96(20):203112.
- [29] SEOL J H, JO I, MOORE A L, et al. Two-dimensional phonon transport in supported graphene[J]. *Science*, 2010, 328(5975):213-216.
- [30] JANG W, CHEN Z, BAO W, et al. Thickness-dependent thermal conductivity of encased graphene and ultrathin graphite[J]. *Nano Letters*, 2010, 10(10):3909-3913.
- [31] PETTES M T, JO I, YAO Z, et al. Influence of polymeric residue on the thermal conductivity of suspended bilayer graphene[J]. *Nano Letters*, 2011, 11(3):1195-1200.
- [32] CHEN S, WU Q, MISHRA C, et al. Thermal conductivity of isotopically modified graphene[J]. *Nature Materials*, 2012, 11(3):203-207.
- [33] XU Z, LIU Y J, ZHAO X L, et al. Ultrastiff and strong graphene fibers via full-scale synergetic defect engineering[J]. *Advanced Materials*, 2016, 28(30):6449-6456.
- [34] XIN G Q, YAO T K, SUN H T, et al. Highly thermally conductive and mechanically strong graphene fibers[J]. *Science*, 2015, 349(6252):1083-1087.
- [35] FANG B, CHANG D, XU Z, et al. A review on graphene fibers: expectations, advances, and prospects[J]. *Advanced Materials*, 2020, 32(5):e1902664.
- [36] PARK H, LEE K H, KIM Y B, et al. Dynamic assembly of liquid crystalline graphene oxide gel fibers for ion transport[J]. *Science Advances*, 2018, 4:2104.
- [37] XIN G, ZHU W, DENG Y, et al. Microfluidics-enabled orientation and microstructure control of macroscopic graphene fibres[J]. *Nature Nanotechnology*, 2019, 14(2):168-175.
- [38] LI Z, LIU Z, SUN H Y, et al. Superstructured assembly of nanocarbons: fullerenes, nanotubes, and graphene[J]. *Chemical Reviews*, 2015, 115(15):7046-7117.
- [39] XU W N, ZHAO Q, CHEN C T, et al. Ultrathin thermoresponsive self-folding 3D graphene[J]. *Science Advances*, 2017, 3:e1701084.
- [40] PENG L, XU Z, LIU Z, et al. Ultrahigh thermal conductive yet superflexible graphene films[J]. *Advanced Materials*, 2017, 29(27):1700589.
- [41] WANG N, SAMANI M K, LI H, et al. Tailoring the thermal and mechanical properties of graphene film by structural engineering[J]. *Small*, 2018, 14(29):1801346.
- [42] ZOU R, LIU F, HU N, et al. Carbonized polydopamine nanoparticle reinforced graphene films with superior thermal conductivity[J]. *Carbon*, 2019, 149:173-180.
- [43] WU X, LI H, CHENG K, et al. Modified graphene/polyimide composite films with strongly enhanced thermal conductivity[J]. *Nanoscale*, 2019, 11(17):8219-8225.
- [44] WANG Y J, XIA S, LI H, et al. Unprecedentedly tough, folding-endurance, and multifunctional graphene-based artificial na-re with predesigned 3D nanofiber network as matrix[J]. *Advanced Functional Materials*, 2019, 29(38):1903876.
- [45] FENG C P, CHEN L B, TIAN G L, et al. Multifunctional thermal management materials with excellent heat dissipation and generation capability for future electronics[J]. *ACS Applied Materials & Interfaces*, 2019, 11(20):18739-18745.
- [46] RENTERIA J D, RAMIREZ S, MALEKPOUR H, et al. Strongly anisotropic thermal conductivity of free-standing reduced graphene oxide films annealed at high temperature[J]. *Advanced Functional Materials*, 2015, 25(29):4664-4672.
- [47] CHEN S J, WANG Q L, ZHANG M M, et al. Scalable production of thick graphene film for next generation thermal management application[J]. *Carbon*, 2020, 167:270-277.
- [48] LIN S F, JU S, ZHANG J W, et al. Ultrathin flexible graphene films with high thermal conductivity and excellent EMI shielding performance using large-sized graphene oxide flakes[J]. *RSC Advances*, 2019, 9(3):1419-1427.
- [49] SHEN B, ZHAI W T, ZHENG W G. Ultrathin flexible graphene film: an excellent thermal conducting material with efficient EMI shielding[J]. *Advanced Functional Materials*, 2014, 24(28):4542-4548.
- [50] WANG B, CUNNING B V, KIMN Y, et al. Ultrastiff, strong, and highly thermally conductive crystalline graphitic films with mixed stacking order[J]. *Advanced Materials*, 2019, 31(29):e1903039.
- [51] ZENG Y Q, LI T, YAO Y G, et al. Thermally conductive reduced graphene oxide thin films for extreme temperature sensors[J]. *Advanced Functional Materials*, 2019, 22(22):1901388.
- [52] GUO Y, DUN C C, XU J W, et al. Ultrathin, washable, and large-area graphene papers for personal thermal management[J]. *Small*, 2017, 13(44):1702645.
- [53] VU M C, THI T N A, LIM J H, et al. Ultrathin thermally conductive yet electrically insulating exfoliated graphene fluoride film for high performance heat dissipation[J]. *Carbon*, 2020, 157:741-749.
- [54] LUO F B, WU K, SHI J, et al. Green reduction of graphene oxide by polydopamine to a construct flexible film: superior flame retardancy and high thermal conductivity[J]. *Journal of Materials Chemistry A*, 2017, 5(35):18542-18550.
- [55] WANG X W, WU P Y. Highly thermally conductive fluorinated graphene films with superior electrical insulation and mechanical flexibility[J]. *ACS Applied Materials & Interfaces*, 2019, 11(24):21946-21954.
- [56] CAO R R, WANG Y Z, CHEN S, et al. Multiresponsive shape-stabilized hexadecyl acrylate-grafted graphene as a phase change material with enhanced thermal and electrical conductivities[J]. *ACS Applied Materials & Interfaces*, 2019, 11(9):8982-8991.
- [57] MENG X, PAN H, ZHUC L, et al. Coupled chiral structure in graphene-based film for ultrahigh thermal conductivity in both

- in-plane and through-plane directions[J]. ACS Applied Materials & Interfaces, 2018, 10(26):22611-22622.
- [58] SONG N, JIAO D J, DING P, et al. Anisotropic thermally conductive flexible films based on nanofibrillated cellulose and aligned graphene nanosheets[J]. Journal of Materials Chemistry C, 2016, 4(2):305-314.
- [59] SONG N, JIAO D J, CUI S Q, et al. Highly anisotropic thermal conductivity of layer-by-layer assembled nanofibrillated cellulose/graphene nanosheets hybrid films for thermal management[J]. ACS Applied Materials & Interfaces, 2017, 9(3):2924-2932.
- [60] SONG N, HOU X H, CHEN L, et al. A green plastic constructed from cellulose and functionalized graphene with high thermal conductivity[J]. ACS Applied Materials & Interfaces, 2017, 9(21):17914-17922.
- [61] ROZADA R, PAREDES J I, VILLAR R, et al. Towards full repair of defects in reduced graphene oxide films by two-step graphitization[J]. Nano Research, 2013, 6(3):216-233.
- [62] GUAN F L, GUI C X, ZHANG H B, et al. Enhanced thermal conductivity and satisfactory flame retardancy of epoxy/alumina composites by combination with graphene nanoplatelets and magnesium hydroxide[J]. Composites Part B, 2016, 98:134-140.
- [63] SONG S H, PARK K H, KIM B H, et al. Enhanced thermal conductivity of epoxy-graphene composites by using non-oxidized graphene flakes with non-covalent functionalization [J]. Advanced Materials, 2013, 25(5):732-737.
- [64] ZONG P S, FU J F, CHEN L Y, et al. Effect of aminopropyl-sobutyl polyhedral oligomeric silsesquioxane functionalized graphene on the thermal conductivity and electrical insulation properties of epoxy composites[J]. RSC Advances, 2016, 6(13):10498-10506.
- [65] DING P, SU S S, SONG N, et al. Highly thermal conductive composites with polyamide-6 covalently-grafted graphene by an *in situ* polymerization and thermal reduction process[J]. Carbon, 2014, 66:576-584.
- [66] TANG Z H, KANG H, SHEN Z L, et al. Grafting of polyester onto graphene for electrically and thermally conductive composites[J]. Macromolecules, 2012, 45(8):3444-3451.
- [67] OH H, KIM Y J, KIM J H. Co-curable poly(glycidyl methacrylate)-grafted graphene/epoxy composite for thermal conductivity enhancement[J]. Polymer, 2019, 183:121834.
- [68] TENG C C, MA C C M, LU C H, et al. Thermal conductivity and structure of non-covalent functionalized graphene/epoxy composites[J]. Carbon, 2011, 49(15):5107-5116.
- [69] WANG F Z, DRZAL L T, QIN Y, et al. Mechanical properties and thermal conductivity of graphene nanoplatelet/epoxy composites[J]. Journal of Materials Science, 2014, 50(3):1082-1093.
- [70] ZHU D H, QI Y, YU W, et al. Enhanced Thermal conductivity for graphene nanoplatelets/epoxy resin composites[J]. Journal of Thermal Science and Engineering Applications, 2018, 10(1):011011.
- [71] KIM H S, BAE H S, YU J, et al. Thermal conductivity of polymer composites with the geometrical characteristics of graphene nanoplatelets[J]. Scientific Reports, 2016, 6:26825.
- [72] KUMAR P, YU S, SHAHZAD F, et al. Ultrahigh electrically and thermally conductive self-aligned graphene/polymer composites using large-area reduced graphene oxides[J]. Carbon, 2016, 101:120-128.
- [73] JAROSINSKI L, RYBAK A, GASKA K, et al. Enhanced thermal conductivity of graphene nanoplatelets epoxy composites[J]. Materials Science-Poland, 2017, 35(2):382-389.
- [74] YU A P, RAMESH P, ITKIS M E, et al. Graphite nanoplatelet-epoxy composite thermal interface materials[J]. The Journal of Physical Chemistry C, 2007, 111:7565-7569.
- [75] GUO Y Q, XU G J, YANG X T, et al. Significantly enhanced and precisely modeled thermal conductivity in polyimide nanocomposites with chemically modified graphene *via in situ* polymerization and electrospinning-hot press technology[J]. Journal of Materials Chemistry C, 2018, 6(12):3004-3015.
- [76] CHO E C, HUANG J H, LI C P, et al. Graphene-based thermoplastic composites and their application for LED thermal management[J]. Carbon, 2016, 102:66-73.
- [77] GUO Y Q, YANG X T, RUAN K P, et al. Reduced graphene oxide heterostructured silver nanoparticles significantly enhanced thermal conductivities in hot-pressed electrospun polyimide nanocomposites[J]. ACS Applied Materials & Interfaces, 2019, 11(28):25465-25473.
- [78] QIAN R, YU J H, WU C, et al. Alumina-coated graphene sheet hybrids for electrically insulating polymer composites with high thermal conductivity[J]. RSC Advances, 2013, 3(38):17373-17379.
- [79] CUI X, DING P, ZHUANG N, et al. Thermal conductive and mechanical properties of polymeric composites based on solution-exfoliated boron nitride and graphene nanosheets: a morphology-promoted synergistic effect [J]. ACS Appl Mater Interfaces, 2015, 7(34):19068-19075.
- [80] WANG R, ZHUO D X, WENG Z X, et al. A novel nanosilica/graphene oxide hybrid and its flame retarding epoxy resin with simultaneously improved mechanical, thermal conductivity, and dielectric properties [J]. Journal of Materials Chemistry A, 2015, 3(18):9826-9836.
- [81] YANG J, TANG L S, BAO R Y, et al. Hybrid network structure of boron nitride and graphene oxide in shape-stabilized composite phase change materials with enhanced thermal conductivity and light-to-electric energy conversion capability[J]. Solar Energy Materials and Solar Cells, 2018, 174:56-64.
- [82] ZHANG W B, ZHANG Z X, YANG J H, et al. Largely enhanced thermal conductivity of poly(vinylidene fluoride)/carbon nanotube composites achieved by adding graphene oxide [J]. Carbon, 2015, 90:242-254.
- [83] CHEN J J, CHEN X N, MENG F B, et al. Super-high thermal conductivity of polyamide-6/graphene-graphene oxide composites through *in situ* polymerization[J]. High Performance Polymers, 2016, 29(5):585-594.
- [84] 陈宇, 张代军, 李军, 等. 三维结构石墨烯气凝胶/环氧树脂复合材料的制备和电磁屏蔽性能研究[J]. 材料工程, 2021, 49(5):

- 82-88.
- CHEN Y, ZHANG D J, LI J, et al. Preparation and electromagnetic interference shielding performance research of epoxy composites modified with three-dimensioned graphene aerogels[J]. Journal of Materials Engineering, 2021, 49(5):82-88.
- [85] ALAM F E, DAI W, YANG M H, et al. *In situ* formation of a cellular graphene framework in thermoplastic composites leading to superior thermal conductivity[J]. Journal of Materials Chemistry A, 2017, 5(13):6164-6169.
- [86] WU K, LEI C X, HUANG R, et al. Design and preparation of a unique segregated double network with excellent thermal conductive property [J]. ACS Applied Materials & Interfaces, 2017, 9(8):7637-7647.
- [87] YANG J, LI X F, HAN S, et al. Air-dried, high-density graphene hybrid aerogels for phase change composites with exceptional thermal conductivity and shape stability[J]. Journal of Materials Chemistry A, 2016, 4(46):18067-18074.
- [88] AN F, LI X F, MIN P, et al. Vertically aligned high-quality graphene foams for anisotropically conductive polymer composites with ultrahigh through-plane thermal conductivities [J]. ACS Appl Mater Interfaces, 2018, 10(20):17383-17392.
- [89] FANG H M, GUO H C, HU Y R, et al. *In-situ* grown hollow Fe₃O₄ onto graphene foam nanocomposites with high EMI shielding effectiveness and thermal conductivity[J]. Composites Science and Technology, 2020, 188:107975.
- [90] LIU J, LIU Y F, ZHANG H B, et al. Superelastic and multi-functional graphene-based aerogels by interfacial reinforcement with graphitized carbon at high temperatures[J]. Carbon, 2018, 132:95-103.
- [91] ZHANG F, FENG Y Y, QIN M M, et al. Stress controllability in thermal and electrical conductivity of 3D elastic graphene-crosslinked carbon nanotube sponge/polyimide nanocomposite [J]. Advanced Functional Materials, 2019, 29(25):1901383.
- [92] MIN P, LIU J, LI X F, et al. Thermally conductive phase change composites featuring anisotropic graphene aerogels for real-time and fast-charging solar-thermal energy conversion[J]. Advanced Functional Materials, 2018, 28(51):1805365.
- [93] WU Z, XU C, MA C, et al. Synergistic effect of aligned graphene nanosheets in graphene foam for high-performance thermally conductive composites[J]. Advanced Materials, 2019, 31(19):1900199.
- [94] LIAO H H, CHEN W H, LIU Y, et al. A phase change material encapsulated in a mechanically strong graphene aerogel with high thermal conductivity and excellent shape stability[J]. Composites Science and Technology, 2020, 189:108010.
- [95] DAI W, YU J H, WANG Y, et al. Enhanced thermal conductivity for polyimide composites with a three-dimensional silicon carbide nanowire@graphene sheets filler[J]. Journal of Materials Chemistry A, 2015, 3(9):4884-4891.
- [96] LIANG C B, QIU H, HAN Y Y, et al. Superior electromagnetic interference shielding 3D graphene nanoplatelets/reduced graphene oxide foam/epoxy nanocomposites with high thermal conductivity[J]. Journal of Materials Chemistry C, 2019, 7(9):2725-2733.
- [97] LIU Z, CHEN Y, LI Y, et al. Graphene foam-embedded epoxy composites with significant thermal conductivity enhancement [J]. Nanoscale, 2019, 11(38):17600-17606.
- [98] QIN M M, XU Y X, CAO R, et al. Efficiently controlling the 3D thermal conductivity of a polymer nanocomposite *via* a hyperelastic double-continuous network of graphene and sponge [J]. Advanced Functional Materials, 2018, 28(45):1805053.
- [99] YANG J, QI G Q, LIU Y, et al. Hybrid graphene aerogels/phase change material composites: thermal conductivity, shape-stabilization and light-to-thermal energy storage[J]. Carbon, 2016, 100:693-702.
- [100] YANG J, ZHANG E W, LI X F, et al. Cellulose/graphene aerogel supported phase change composites with high thermal conductivity and good shape stability for thermal energy storage [J]. Carbon, 2016, 98:50-57.
- [101] ZHANG Y F, HAN D, ZHAO Y H, et al. High-performance thermal interface materials consisting of vertically aligned graphene film and polymer[J]. Carbon, 2016, 109:552-557.
- [102] LI Q, GUO Y F, LI W W, et al. Ultrahigh thermal conductivity of assembled aligned multilayer graphene/epoxy composite [J]. Chemistry of Materials, 2014, 26(15):4459-4465.
- [103] JUNG H, YU S, BAE N S, et al. High through-plane thermal conduction of graphene nanoflake filled polymer composites melt-processed in an L-shape kinked tube[J]. ACS Appl Mater Interfaces, 2015, 7(28):15256-15262.
- [104] LI Y, WEI W, WANG Y, et al. Construction of highly aligned graphene-based aerogels and their epoxy composites towards high thermal conductivity[J]. Journal of Materials Chemistry C, 2019, 7(38):11783-11789.
- [105] HAO H, WEN D, YAN Q W, et al. Graphene size-dependent modulation of graphene frameworks contributing to the superior thermal conductivity of epoxy composites[J]. Journal of Materials Chemistry A, 2018, 6(25):12091-12097.

基金项目:国家自然科学基金项目(51802296);北京市科技计划资助项目(Z191100005619006)

收稿日期:2020-10-09; **修订日期:**2021-01-18

通讯作者:郭建强(1980—),男,工程师,博士,研究方向为石墨烯聚合物复合材料,联系地址:北京市81信箱2分箱(100095),E-mail:guo-jianqiang2010@163.com

(本文责编:高磊)